Simultaneous Measurement of Implosion Process and Heating Laser Injection by Using X-ray Framing Camera

Mayuko KOGA, Takashi FUJIWARA, Tatsuhiro SAKAIYA, Myongdok LEE, Keisuke SHIGEMORI, Hiroyuki SHIRAGA, Hiroshi AZECHI, and Tetsuo Ozaki*

Institute of Laser Engineering, Osaka University, 2-6 Yamada-Oka, Suita, Osaka 565-0871, Japan

**National Institute for Fusion Science, 322-6, Oroshi-cho, Toki, Gifu 509-5292, Japan*

(Received: 1 September 2008 / Accepted: 25 December 2008)

In fast ignition experiment, it is important for effective heating of imploded core to control the injection time of heating laser synchronized with imploded core formation. However, it is difficult to measure the imploded core and heating laser injection at the same time. In this paper, we propose the simultaneous measurement using X-ray framing camera (XFC). In implosion experiment without heating laser, we observed only 2D thermal X-ray images of imploded core. On the other hand, in implosion experiments with heating laser, not only 2D X-ray images but also bright zones were observed on striplines. This zone is considered to show high energy X-ray from hot electron heated by heating laser. It is considered that the heating laser injection time is estimated from the peak position of this bright X-ray intensity profile. To explain the broad X-ray intensity profile, MCP gain calculation is improved by including the energy distribution of secondary electrons. The calculated results show better correspondence to experimental data. Although the detailed X-ray energy measurement is needed, it is considered that we can estimate heating laser injection time with about 10 ps resolution from the peak position of high energy X-ray intensity profile.

Keywords: fast ignition, x-ray framing camera, x-ray imaging, hard x-ray, micro channel plate, dynode model

1. Introduction

Fast ignition [1-4] is one of the proposed ways to generate fusion plasmas. This scheme separates lasers into two systems: one for implosion and the other for heating the imploded fuel core. Fast ignition scheme is considered as a powerful method for generating laser fusion plasma because the laser energy required for implosion in fast ignition scheme is expected to be much smaller than that in the central ignition scheme. For efficient heating of the imploded core, it is necessary to control a heating laser injection time synchronized with imploded core. However, the large spectral difference between thermal X-ray from the imploded core plasma and high energy X-ray from hot electrons generated by the heating laser causes difficulty in measuring both X-rays at the same time. In this study, we report a simultaneous measurement of both X-rays and discuss the possibility of heating laser injection time measurement with an X-ray framing camera (XFC).

2. Experiment

X-ray framing cameras have been widely used for diagnosing laser-driven implosions [5-8]. Figure 1 shows the schematic diagram of our X-ray framing camera system made by Hamamatsu photonics, Model C5896. The X-ray framing camera has two micro channel plates (MCP) which size is 40 mm × 50 mm. The first MCP is for gating and the second MCP is for amplification of a signal. Four Au striplines are deposited on the first MCP. Four electric pulses propagate along each stripline. The first MCP becomes sensitive only when electric pulses exists, therefore time evolution of X-ray intensity is recorded along striplines. The full width at half maximum (FWHM) of electric pulses is 360 ps and the peak voltage is 680 V, the propagating speed is 1.6×10^8 m/s. Electrons through tandem MCP hit the fluorescence plate and the visible fluorescent lights are recorded with a CCD camera (Hamamatsu photonics, C4742-95-12ER, 512 pixel × 672 pixel). 2-D X-ray images of core plasma are made on the striplines with a pinhole imager plate. The diameter of the pinholes is 15 μm and the magnification is 5. 3×4 pinholes are fabricated on a 50 μm thick Pt imager plate. Three images are recorded with 80 ps time interval in each stripline. The time interval of four striplines is set for 500 ps.

The experiments were performed using Gekko XII laser system and Peta Watt (PW) laser system at the Institute of Laser Engineering, Osaka University. 9 beams (400 J/beam) of Gekko XII irradiated the plastic shell target to create the imploded core plasma and after that an ultra-intense PW laser (200 J) were injected to heat the core plasma. The pulse width of PW laser is about 0.8 ps.

author's e-mail: koga-m@ile.osaka-u.ac.jp

The targets were deuterated polystyrene shells (about 500 μm in diameter and 6 μm in thickness) with Au cones, which had a 30° opening angle. The tip of the cone was placed 50 μm away from the target center. Observation was made in the direction perpendicular to the Au cone. An X-ray streak camera (XSC) coupled to a slit camera was simultaneously used to measure the imploded core plasma.

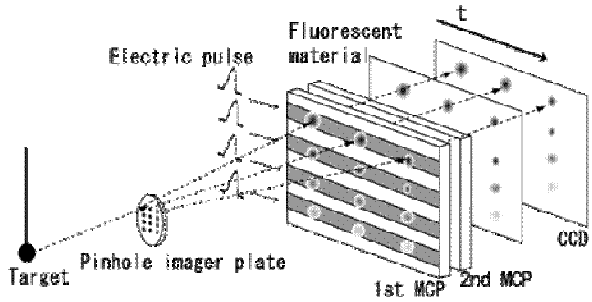

Fig.1 The schematic diagram of our X-ray framing camera.

3. Results and discussion

In previous work, the availability of X-ray framing camera is clarified [9]. The core plasma radius estimated from X-ray framing camera images is consistent with that estimated from X-ray streak camera images and agrees well with the result of 1D simulation. This means that the spatial resolution of X-ray framing camera is good enough to observe implosion processes.

Figure 2 shows the time- and space-resolved images obtained by X-ray framing camera (shot number 29984). As shown in Fig. 2, bright zones are observed in second and third stripline. The bright zones were observed only when PW laser was injected. Thus, it is considered that the high energy X-ray due to hot electrons generated by PW laser passed through the pinhole imager plate and made these bright zones. The transmission of 50 μm thick Pt plate is 1/e when the incident X-ray energy is about 45 keV. Therefore, the energy of X-ray passing through pinhole imager plate is considered to be roughly above 50 keV. The bright, short pulse width line similar to X-ray framing camera was also recorded in the X-ray streak camera image.

The temporal evolution of X-ray intensity profile reconstructed from the X-ray image is shown in Fig. 3. The gray line shows the experimental data and the black line shows a Gaussian profile with FWHM of 200 ps. It is clearly seen that the measured X-ray intensity fits in well with the Gaussian profile. In Fig. 3, the dotted vertical line shows the time when the bright line was observed by X-ray streak camera. It is clearly seen that the timing almost agrees with the fitted X-ray peak position of X-ray framing camera. In the experiment shown in Fig. 3 (b), the injection time of PW laser is delayed 250 ps compared to the experiment shown in Fig. 3 (a). It is found that the X-ray

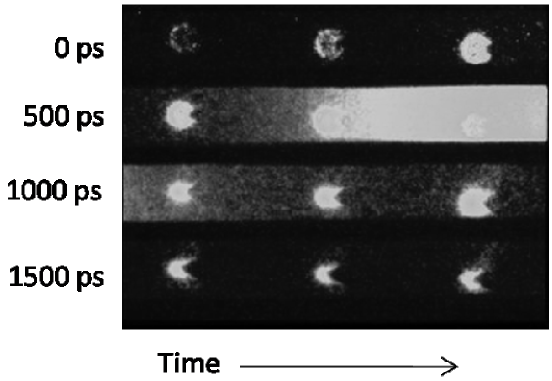

Fig.2 The time- and space-resolved images obtained by X-ray framing camera (shot number 29984).

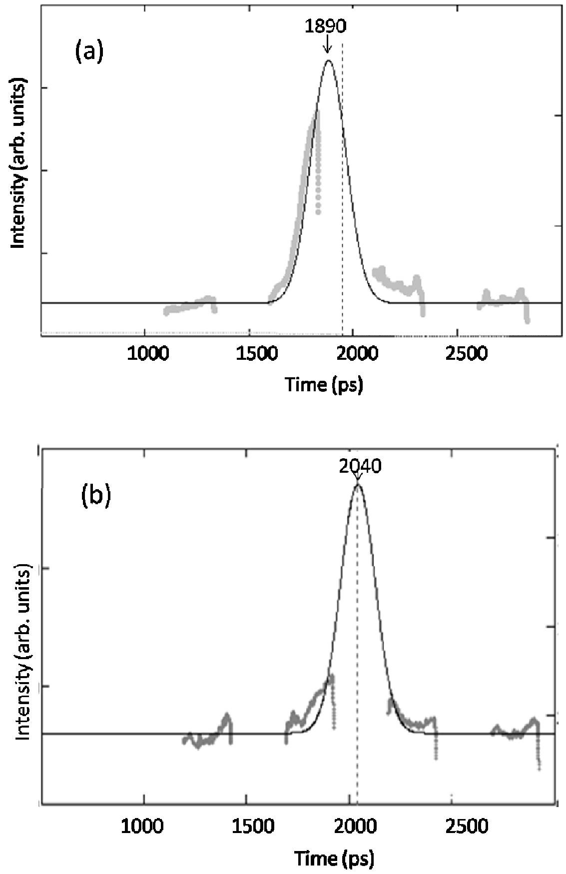

Fig.3 The temporal evolution of X-ray intensity. The gray line shows experimental data. The black line is the calculated X-ray intensity assuming Gaussian profiles. The dotted vertical line shows the time when the bright line was observed by X-ray streak camera. Fig. 3 (a) and (b) show the result of shot number 29984 and 29986 respectively. The PW laser injection time in Fig. 3 (b) was delayed 250 ps compared to Fig. 3 (a).

peak position is about 150 ps delayed compared with Fig. 3 (a). The laser injection time is considered to have an error bar less than 100 ps due to jitter. Therefore, we consider that we can estimate the heating laser injection time from the peak position of high energy X-ray intensity profile

The time resolution of our X-ray framing camera system is considered to be about 100 ps. However, as shown in Fig. 2 and Fig. 3, the high energy X-ray image shows broad bright zone over 200 ps, although the pulse width of PW laser is only about 0.8 ps. This degradation of time resolution cannot be explained by the simple dynode model used in thermal X-ray experiment. Therefore, we are trying to build the new model which explains this broadening.

The concept of dynode model is shown in Fig. 4. One dynode is defined by electrons traveling one side wall to the other side wall of the channel. One dynode gain δ is defined as follows [10];

$$\delta = \left(V_z / V_c\right) \cdot k \qquad (1)$$

Here, Vz is the voltage between one dynode, Vc is the first crossover potential (i.e., the minimum potential for unity secondary emission ratio) and k is a constant efficient. The total MCP gain G of n dynodes is the multiplication of all dynode's gain.

$$G = \delta_1 \cdot \delta^{k(n-1)} \qquad (2)$$

Here δ_1 is gain of the first input electron.

In thermal X-ray measurement, n is typically fixed at about 9.8 and δ is considered to be proportional to the applied electric pulse voltage. This nonlinear gain response makes the high temporal resolution measurement possible. For example, time resolution of X-ray framing camera becomes about $360/n^{0.5}$=115 ps when FWHM of electric pulses is 360 ps. However, in this experiment, high energy X-ray (≳ 50 keV) may pass through Pt pinhole imager plate and penetrate MCP generating electrons throughout the MCP channel shown in Fig. 4. Electrons generated in mid MCP channel have smaller n compared to that of electrons generated on MCP channel surface. This decrease of n may cause the degradation of time resolution. In previous paper [9], we confirmed this concept by calculation in fixed secondary electron energy (2 eV). Here we try to improve the calculation by including energy distribution of secondary electrons. The energy distribution function of secondary electrons is assumed as the following probability function [11];

$$f(E) = C \cdot \exp\left\{ -\left[\ln \frac{E}{E_0}\right] / 2\sigma^2 \right\} \qquad (3)$$

, where the most probable energy E_0=2.3eV and σ=0.6. As shown in Fig. 5, the value for E_0 and σ is chosen to match experimental data of Ref [12]. In calculation, the thickness of MCP was set at 480 μm, the diameter of one channel was set at 12 μm. The electric pulse was set at

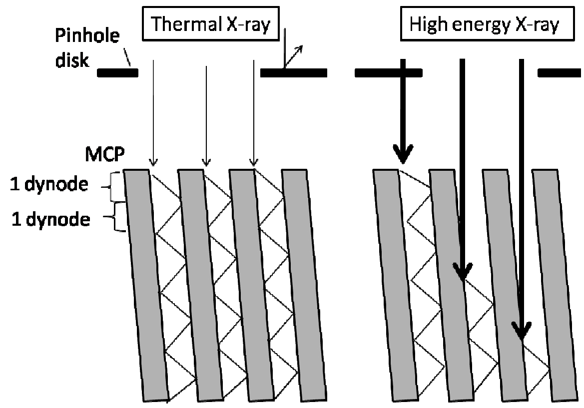

Fig.4 The left figure shows the concept of simple dynode model. The right figure shows the new model including the effect of high energy X-ray.

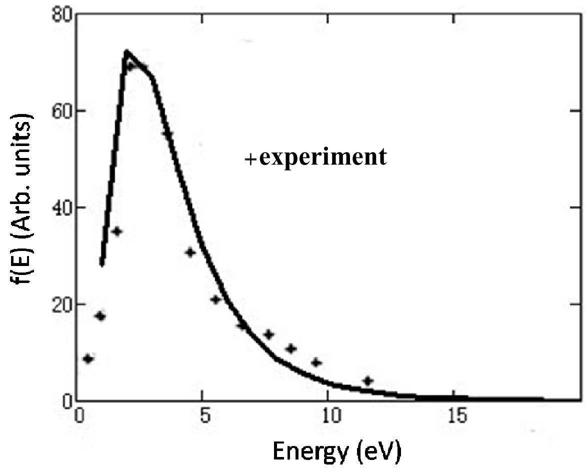

Fig.5 The assumed energy distribution function of secondary electrons. The experimental points are from Ref. [12].

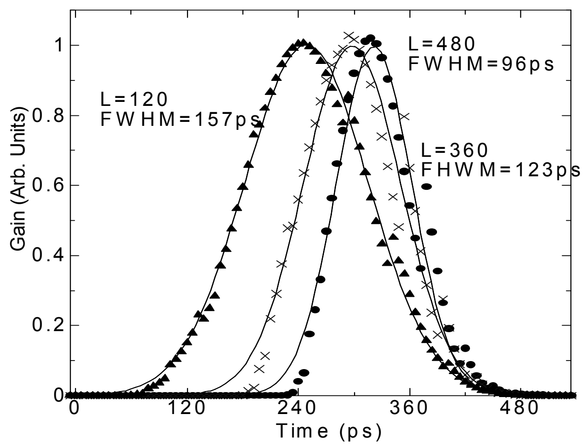

Fig.6 The calculated results. L means the distance where electrons propagate.

680V at peak, 360 ps at FWHM, and its propagation speed was set at 1.6×10^8 m/s. These parameters were based on factory data of Hamamatsu photonics. Other parameters are set using examples from ref [10]. Electrons penetrate MCP within 100 impacts were counted as gain. Figure 6 shows the calculated results. The horizontal axis shows the time converted from the position of stripline. The vertical axis shows the gain, however calculated gains are normalized. These profiles are equal to gate profiles and mean time resolutions of X-ray framing camera. The gain of electrons generated on MCP surface means the thermal X-ray experiments case. The time resolution of that case, 96 ps, is agrees better with the experimental data compared to that in the previous calculation. It is found that gate profile of electrons generated in mid MCP channel (L=240, 360) is wider than that of electrons generated on MCP surface (L=480). This result is considered to explain the broad high energy X-ray profile qualitatively. It is found that electrons generated in mid MCP affect not only degradation of time resolution but also the detected peak position. Therefore, now we are trying to obtain more data such as injecting X-ray energy distribution for constructing more accurate fitting model. We think that the accurate fitting model will solve the problem of degradation of time resolution and change of peak position. We will be able to estimate the injection time of heating laser with about 10 ps resolution from the peak position of X-ray intensity using accurate fitting model.

4. Summary

We succeeded in measuring PW laser injection time and the imploded core plasma simultaneously by using X-ray framing camera. PW laser injection time was observed as bright zones on striplines. The measured X-ray intensity profiles fit with Gaussian profiles. The peak position of fitted X-ray intensity is almost in agreement with the time when the bright lines was observed by X-ray streak camera. Moreover, the peak position is found to delay corresponding to the delayed setting of PW injection time. MCP gain of high energy X-ray was calculated by using dynode model and the assumed energy distribution function of secondary electrons. It is found that the calculated results shows the good agreement with experimental data and explains the broadening of high energy X-ray intensity profile qualitatively. It is concluded that we will be able to estimate heating laser injection time with about 10 ps accuracy from the peak position of X-ray intensity recorded by X-ray framing camera.

5. References

[1] N. G. Basov, S. Yu. Gus'kov, and L. P. Feoktistov, J. Soviet Laser Research **13**, 396 (1992).

[2] M. Tabak, J. Hammer, M. E. Glinsky, W. L. Kruer, S. C. Wilks, J. Woodworth, E. M. Campbell, and M. D. Perry, Phys. Plasmas **1**, 1626 (1994).

[3] R. Kodama, P. A. Norreys, K. Mima, A. E. Dangor, R. G. Evans, H. Fujita, Y. Kitagawa, K. Krushelnick, T. Miyakoshi, N. Miyanaga et al., NATURE **412**, 798 (2001).

[4] R. Kodama, H. Shiraga, K. Shigemori, Y. Toyama, S. Fujioka, H. Azechi, H. Fujita, H. Habara, T. Hall, Y. Izawa et al., NATURE **418**, 933 (2002).

[5] D. K. Bradley, P. M. Bell, J. D. Kilkenny, R. Hanks, O. Landen, P. A. Jaanimagi, P. W. McKenty, and C. P. Verdon, Rev. Sci. Instrum. **63**, 4813 (1992).

[6] J. D. Kilkenny, Rev. Sci. Instrum. **63**, 4688 (1992).

[7] D. K. Bradley, P. M. Bell, O. L. Landen, J. D. Kilkenny, and J. Oertel, Rev. Sci. Instrum. **66**: 716 (1995).

[8] M. Katayama, M. Nakai, T. Yamanaka, Y. Izawa, and S. Nakai, Rev. Sci. Instrum. **62**, 124 (1991).

[9] Mayuko Koga,∗ Takashi Fujiwara, Tatsuhiro Sakaiya, Myongdok Lee, Keisuke Shigemori, Hiroyuki Shiraga, and Hiroshi Azechi, Rev. Sci. Instrum., to be published.

[10] Edward H. Eberhardt, Applied Optics, **18**, 1418 (1979).

[11] J. J. Scholtz, D. Dijkkamp, R. W. A. Schmitz, Philips Journal of Research: **50,** 375 (1996).

[12] A. Authinarayanan and R. W. Dudding, Advan. Electron. Electron. Phys., **A 40,** 167 (1976)